Molecular Crystals and Liquid Crystals Science and Technology. Section A. Molecular Crystals and Liquid Crystals

Publication details, including instructions for authors and subscription information:
http://www.tandfonline.com/loi/gmcl19

Magnetic and Electric Field Induced Periodic Deformations in Nematics-Effect of Director Pretilt

U. D. Kini [a]

[a] Raman Research Institute, Bangalore, 560 080, India

Version of record first published: 04 Oct 2006.

To cite this article: U. D. Kini (1996): Magnetic and Electric Field Induced Periodic Deformations in Nematics-Effect of Director Pretilt, Molecular Crystals and Liquid Crystals Science and Technology. Section A. Molecular Crystals and Liquid Crystals, 289:1, 181-206

To link to this article: http://dx.doi.org/10.1080/10587259608042321

Mol. Cryst. Liq. Cryst., 1996, Vol. 289, pp. 181–206
Reprints available directly from the publisher
Photocopying permitted by license only

Magnetic and Electric Field Induced Periodic Deformations in Nematics-Effect of Director Pretilt

U. D. KINI

Raman Research Institute, Bangalore-560 080, India

(Received 16 January 1996; In final form 13 June 1996)

Using linear stability analysis, theoretical studies are reported on the formation of static periodic distortions (PD) in a nematic sample under the action of crossed electric (**E**) and magnetic (**H**) fields applied on a uniformly aligned initial director configuration ($\mathbf{n}_0$). With the rigid anchoring hypothesis, results for director pretilt away from the homeotropic ($\phi_o \neq 0$) reduce to those previously obtained for homeotropic alignment as a special case. Variation of magnetic tilt may lead to discontinuous change in the wavevector of PD. Increase of ϕ_o quenches PD in favour of the aperiodic or homogeneous deformation (HD). Phase diagrams are presented for PD occurring in nematic materials with different types of susceptibility anisotropy.

1. INTRODUCTION

The continuum theory [1–4] has provided reasonably complete explanations for many interesting effects observed under the actions of **E** and **H** fields on nematic samples. Apart from the aperiodic or homogeneous deformation (HD), periodic distortions (PD) are also known to occur in various geometries [5–8]. Explanations for these phenomena have been provided [12] by the use of the continuum theory taking into account possible effects of flexoelectricity [9], director pretilt and weak anchoring at the boundaries [10], effect of obliquely applied fields [11], etc.

The application of a transverse high frequency *ac* **E** field in the bend Freedericksz geometry causes HD above a first order transition [13, 14] in a nematic (such as 5CB) having high, posititve dielectric anisotropy (ε_A) and

positive diamagnetic anisotropy (χ_A); with a strong stabilizing **H** along $\mathbf{n}_0$, the deformation above threshold becomes periodic [14, 15]. This is a typical example of the action of crossed **E** and **H** fields [11, 16]. Different models have been proposed [17, 18] to explain the occurrence of PD. The linear perturbation model [18] captures qualitatively some of the aspects of PD found experimentally [14, 15].

Nematic materials such as $M1$ [19] and CCH-7 [20] are also interesting as their susceptibility anisotropies have opposite signs. In these materials, the geometry involving strong stabilizing and destabilizing fields can be duplicted but the relative directions of **E** and **H** will be different from those studied in refs. [13–18]. The technique of ref. [18] along with rigid anchoring hypothesis can be employed to show that PD may occur in these materials under the action of crossed fields [21]. The periodicity wavevector in the sample plane may change continuously or discontinuously depending upon material parameters; in some cases, PD may be suppressed over a range of magnetic tilts. In ref. [21], only the homeotropic initial alignment is considered. It should be interesting to study the effect of director pretilt on the phase diagrams of different PD modes.

The above stated reasons form the motivation behind the present endeavour. In section 2, the governing equations of ref. [21] are briefly restated along with the boundary conditions for the rigid anchoring hypothesis and the HD thresholds are worked out for different materials. In section 3 the PD thresholds and periodicities are obtained numerically as functions of different parameters for $M1$; section 4 describes similar studies on 5CB. Section 5 concludes the communication by summarizing the main results.

2. GOVERNING EQUATIONS, BOUNDARY CONDITIONS

A nematic insulator of thickness $2h$ is confined between glass plates $z = \pm h$ and sandwiched between flat electrodes $x = \pm g$ lying in the yz plane. The electrode gap $2g$ is assumed to be large compared to the sample thickness $2h$ and the sample is studied near $x = 0$, midway between the electrodes. The initial director orientation is uniform in the yz plane such that

$$\mathbf{n}_0 = (0, S, C); S = \sin \phi_o, C = \cos \phi_o; \phi_o = \text{constant}; \tag{1}$$

i.e., *homeotropic* for ($\phi_o = 0$) and *homogeneous* or *planar* for ($\phi_o = \pi/2$). **H** is either along $\mathbf{n}_0$,

$$\mathbf{H}_\parallel = (0, H_\parallel S, H_\parallel C) \tag{2}$$

or in a plane normal to $\mathbf{n}_0$,

$$\mathbf{H}_\perp = (H_\perp C_\alpha, H_\perp S_\alpha C, -H_\perp S_\alpha S); \tag{3}$$

where $S_\alpha = \sin\alpha$ and $C_\alpha = \cos\alpha$. When $\alpha = 0$, $\mathbf{H}_\perp$ is along x, while for $\alpha = \pi/2$, it is in the yz plane. For general values of ϕ_o, $\mathbf{H}_\perp$ lies along x only for $\alpha = 0$. The unperturbed $\mathbf{E}$ field $\mathbf{E}_0 = (E_{xo}, 0, 0)$ inside the sample is uniform with $E_{xo} = V_o/2g$ where V_o is the potential difference applied between the electrodes. Under perturbations, the director and $\mathbf{E}$ fields become

$$\mathbf{n} = [\sin\theta, \cos\theta\sin(\phi_o + \phi), \cos\theta\cos(\phi_o + \phi)];$$

$$\mathbf{E} = \mathbf{E}_0 + \mathbf{E}'; \mathbf{E}' = -\nabla\psi \tag{4}$$

where the perturbations θ, ϕ, ψ are functions of x, y, z; Maxwell's curl equation enables writing $\mathbf{E}'$ as the gradient of the scalar potential ψ. For linear perturbations, the total free energy density (at fixed voltage between electrodes) is

$$F = \frac{1}{2}[K_1(\theta_{,x} + C\phi_{,y} - S\phi_{,z})^2 + K_2(\phi_{,x} - C\theta_{,y} + S\theta_{,z})^2$$

$$+ K_3\{(S\theta_{,y} + C\theta_{,z})^2 + (S\phi_{,y} + C\phi_{,z})^2\}$$

$$- \frac{1}{4\pi}\{\varepsilon_\perp(\psi_{,x}^2 + \psi_{,y}^2 + \psi_{,z}^2) + \varepsilon_A(E_{x0}\theta - S\psi_{,y} - C\psi_{,z})^2\}] + f_M;$$

$$f_M = \frac{\chi_A H_\parallel^2}{2}(\theta^2 + \phi^2) \text{ if } H_\perp = 0;$$

$$f_M = -\frac{\chi_A H_\perp^2}{2}(C_\alpha\theta + S_\alpha\phi)^2 \text{ if } H_\parallel = 0 \tag{5}$$

where K_1, K_2 and K_3 are the splay, twist and bend elastic constants, respectively; $\varepsilon_\parallel, \varepsilon_\perp$ are, respectively, the dielectric constants parallel to and normal to the director; a subscripted comma denotes partial differentiation. The value of the magnetic term f_M depends on the $\mathbf{H}$ field chosen. Maxwell's divergence equation results by minimizing the total free energy with respect

to ψ holding other quantities constant:

$$\operatorname{div}(\mathbf{D}) = -[\varepsilon_\perp \psi_{,xx} + (\varepsilon_\perp + \varepsilon_A S^2)\psi_{,yy} + 2\varepsilon_A SC\psi_{,yz} + (\varepsilon_\perp + \varepsilon_A C^2)\psi_{,zz}] + \varepsilon_A E_{xo}(S\theta_{,y} + C\theta_{,z}) = 0 \tag{6}$$

where **D** is the electric displacement. With ψ constant, the torque equations result through variations of θ, ϕ:

$$K_1\theta_{,xx} + (K_2C^2 + K_3S^2)\theta_{,yy} + (K_2S^2 + K_3C^2)\theta_{,zz} + 2(K_3 - K_2)SC\theta_{,yz} + \theta\left(\frac{\varepsilon_A E_{xo}^2}{4\pi} + a_\theta\right) + a_\phi\phi + (K_1 - K_2)(\phi_{,xy}C - \phi_{,xz}S) - \frac{\varepsilon_A E_{xo}}{4\pi}(\psi_{,y}S + \psi_{,z}C) = 0 \tag{7}$$

$$K_2\phi_{,xx} + (K_1C^2 + K_3S^2)\phi_{,yy} + (K_3C^2 + K_1S^2)\phi_{,zz} + 2(K_3 - K_1)SC\phi_{,yz} + b_\phi\phi + b_\theta\theta + (K_1 - K_2)(\theta_{,xy}C - \theta_{,xz}S) = 0 \tag{8}$$

$$a_\theta = \chi_A H_\perp^2 C_\alpha^2 \text{ and } a_\phi = \chi_A H_\perp^2 S_\alpha C_\alpha; \text{ or } a_\theta = -\chi_A H_\parallel^2 \text{ and } a_\phi = 0;$$

$$b_\phi = \chi_A H_\perp^2 S_\alpha^2 \text{ and } b_\theta = \chi_A H_\perp^2 S_\alpha C_\alpha; \text{ or } b_\phi = -\chi_A H_\parallel^2 \text{ and } b_\theta = 0. \tag{9}$$

By the rigid anchoring hypothesis, the director perturbations must vanish at the sample planes. According to the electromagnetic theory [22], the normal component of the electric displacement is continuous at the sample planes. Inside the sample walls (isotropic dielectric), the E field as well as the induced polarization are along x axis; hence, the z component of the electric displacement vanishes at the sample planes. The boundary conditions become [23]

$$\theta(z = \pm h) = 0;\ \phi(z = \pm h) = 0;$$

$$\varepsilon_A CE_{xo}\theta - \varepsilon_A SC\psi_{,y} - (\varepsilon_\perp + \varepsilon_A C^2)\psi_{,z} = 0 \text{ at } z = \pm h. \tag{10}$$

The next sections consider different solutions of the governing equations (6)–(10) which essentially reduce to an eigenvalue problem. The effect of

flexoelectricity is ignored in (5)–(10). This may be a reasonable assumption if $\mathbf{E}_0$ is an *ac* field with sufficiently high frequency; then, E_{xo} can be identified with the *rms* value. In every case, depending upon the assumptions, a subset of terms from (6)–(10) is chosen for solution. Initially, we put $H_{\parallel} = 0$ and assume that $\mathbf{H}$ acts normal to $\mathbf{n}_0$ as in (3).

The HD threshold is obtained for perturbations depending on only z. In general, all three perturbations are present. The vanishing of θ, ϕ *and* $d\psi/dz$ at the boundaries is the required set of conditions. Noting the modal structure of the equations, we seek solutions of the form

$$(\theta, \phi, \psi) = (\theta_A \cos qz, \phi_A \cos qz, \psi_A \sin qz)$$

where θ_A, ϕ_A *and* ψ_A are constants whose absolute magnitudes are not known; only the ratio of any two of them can be found. The director perturbations are symmetric about the sample centre while the perturbation in the electric potential is antisymmetric. We ignore the uncoupled mode (having higher threshold) in which the perturbations have opposite spatial symmetry. The compatibility of (6)–(8) requires that $q = \pi/2h$ leading to the threshold condition,

$$\left(\frac{\pi}{2}\right)^4 - \omega_1\left(\frac{\pi}{2}\right)^2 + \omega_2 = 0; \omega_1 = \frac{\omega_6}{\omega_4} + h^2\left(\frac{a_\theta}{\omega_4} + \frac{b_\phi}{\omega_5}\right);$$

$$\omega_2 = \frac{b_\phi \omega_6 h^2}{\omega_4 \omega_5}; \omega_3 = \varepsilon_\perp + \varepsilon_A C^2; \omega_4 = K_2 S^2 + K_3 C^2;$$

$$\omega_5 = K_1 S^2 + K_3 C^2; \omega_6 = \frac{\varepsilon_\perp \varepsilon_A E_{xo}^2 h^2}{4\pi \omega_3}. \tag{11}$$

From (11), different threshold fields can be worked out depending upon the material chosen for study. With a stabilizing $\mathbf{E}_0$ applied along x, the magnetic threshold H_F exists with $\mathbf{H}_\perp$ acting normal to $\mathbf{n}_0$ if $\varepsilon_A < 0$ and $\chi_A > 0$:

$$H_F^2 = \frac{H_B^2 \omega_5 (\omega_4 q^2 - \omega_6)}{K_3 (q^2(\omega_5 C_\alpha^2 + \omega_4 S_\alpha^2) - \omega_6 S_\alpha^2)}$$

$$q = \frac{\pi}{2}; H_B = \left(\frac{q}{h}\right)\left(\frac{K_3}{\chi_A}\right)^{1/2}; \tag{12}$$

H_B is the magnetic bend Freedericksz threshold in the absence of $\mathbf{E}_0$. Clearly, H_F is a function of both the magnetic tilt α and the director prertilt ϕ_o. Similarly, in a material with $\chi_A < 0$, $\varepsilon_A > 0$ and a stabilizing $\mathbf{H}_\perp$ field, one can find the electric threshold for *HD*:

$$E_F^2 = \frac{E_B^2 \omega_3(\omega_4\omega_5 q^2 - K_3\omega_7(\omega_5 C_\alpha^2 + \omega_4 S_\alpha^2))}{K_3 \varepsilon_\parallel(\omega_5 q^2 - K_3\omega_7 S_\alpha^2)}; q = \frac{\pi}{2};$$

$$\omega_7 = \frac{\chi_A h^2 H_\perp^2}{K_3}; \; E_B = \left(\frac{q}{h}\right)\left(\frac{4\pi K_3 \varepsilon_\parallel}{\varepsilon_A \varepsilon_\perp}\right)^{1/2} \tag{13}$$

In the above, E_B is the electric bend threshold in the absence of $\mathbf{H}_\perp$. Needless to say, E_F is also a function of both α and ϕ_o. The scaling of ε_A by the ratio of dielectric constants is due to the modification of $\mathbf{E}$ inside the sample caused by the director perturbations; this is taken account of via the Maxwell divergence equation and the boundary conditions [13–15, 18].

3. MATERIAL WITH $\varepsilon_A < 0$ AND $\chi_A > 0$

For a material such as *M*1 [19], $\mathbf{H}_\perp$ destabilizes the director orientation while $\mathbf{E}_0$ stabilizes it. Hence, the magnetic threshold for instability is studied as a function of the applied voltage and other parameters. It is convenient to first of all discuss the results for initial homeotropic alignment ($\phi_o = 0$) (for details, see section 3 and Figs. 1–3 of ref. 21) before taking up the case of nonzero director tilt.

3.1. Resume of Results for Homeotropic Orientation $\phi_o = 0$

In the absence of applied fields, $\mathbf{n}_0$ along z defines the axis of cylindrical symmetry for the sample. The application of $\mathbf{E}_0$ along x makes it possible to differentiate between a perturbation in the xz plane (θ) and that in the yz plane (ϕ). The presence of $\mathbf{H}_\perp$ in the xy plane making angle α with x axis breaks the symmetry along another direction and hence makes possible the study of *HD* as well as three distinct *PD* Modes:

xz Mode with periodicity along x; perturbations depend on x and z.

yz Mode with periodicity along y; perturbations depend on y and z.

xyz Mode with periodicity wavevector in the xy plane; perturbations depend on x, y and z.

The case of $\mathbf{H}_\perp$ along $y(\alpha = \pi/2)$ is somewhat special. Here, only HD occurs via a coupling between $\mathbf{H}_\perp$ and ϕ; this deformation grows in the yz plane. It must be remembered that this results from a linear analysis (see section 5). We briefly discuss the nature of the *PD* Modes for other α values.

Consider, for instance, the yz Mode. At sufficiently low magnetic tilt α, solutions of the governing equations will be one of two decoupled kinds having opposite spatial symmetry:

SOLUTION 1 θ, ϕ symmetric, ψ antisymmetric.
SOLUTION 2 θ, ϕ antisymmetric, ψ symmetric.

In general, SOLUTION 1 is studied as it has lower threshold than SOLUTION 2. An obvious reason for this is the higher elastic energy associated with SOLUTION 2. For the yz Mode, the perturbations are found to have the same y dependence of the form $\cos(qy)$ where q is the wavevector of periodicity. The electric perturbations couple only to θ and not to ϕ; E'_z and E'_y have, respectively, a destabilizing and a stabilizing influence on θ. But E'_z is symmetric and E'_y antisymmetric relative to $z = 0$. When the stabilizing $\mathbf{E}_0$ is sufficiently strong, the destabilizing influence of E'_z can make the yz Mode threshold lower than the HD threshold provided that the wavevector q takes an appropriate value, say, q_C. The PD threshold is determined from the minimum of a neutral stability curve (described in section 3.2). A similar argument shows that the xz Mode threshold can also be lower than that of HD.

The next question is, whether it is the xz Mode or the yz Mode that has the lower threshold. When $\mathbf{H}_\perp$ is close to x axis, the yz Mode has lower threshold than the xz Mode as the elastic deformation of the yz Mode is predominantly twist-bend and that of the xz Mode predominantly splay-bend. Rotating $\mathbf{H}_\perp$ away from x axis causes the distortion for either PD Mode to become a mixture of splay, twist and bend. Due to the consequent increase of the splay component in the yz Mode (equivalently, due to an increase of the twist component in the xz Mode), the xz Mode threshold can become lower than that of the yz Mode if α becomes high enough. As PD cannot exist when $\alpha = \pi/2$, even the xz Mode gets quenched when $\mathbf{H}_\perp$ is rotated sufficiently close to the y axis.

For the xyz Mode, the perturbations have the x, y dependence $\sin q(C_\mu x + S_\mu y)$ where μ is the angle between the wavevector and x axis and q the wavevector amplitude. The resulting compatibility condition yields $H_\perp$ as a function of q and μ. The xyz Mode threshold is found as the minimum of a neutral stability surface. In general, this threshold is lower than the HD threshold but is always higher than the xz and yz Mode thresholds; hence,

the xyz Mode is considered to be of only academic interest. It appears that the effect of destabilizing torques cannot cancel the additional elastic stabilizing torques associated with the xyz Mode. Thus, the only Modes of interest are xz and yz.

3.2. Results for $\phi_o \neq 0$

With the above summary, the nature of solutions for the case of a tilted director orientation becomes clear. In this case, $\mathbf{H}_\perp$ (3) is not confined only to the xy plane. Equations (6–8) can no longer support solutions with modal purity; in fact, SOLUTIONS 1 and 2 which are uncoupled for the homeotropic case, get coupled or 'mixed' due to the presence of torques depending on mixed derivatives ($\theta_{,xz}, \phi_{,xz}$, etc). Clearly, higher the director pretilt away from the homeotropic , greater will be the proportion of SOLUTION 2. An obvious effect of the presence of higher distortions is an increase in the xz Mode threshold relative to that of HD (we remember that HD remains modally pure inspite of director pretilt). To study the xz Mode, for instance, solutions are sought such that each perturbation is written as the sum of two terms:

$$\theta(x,z) = \theta_U(z)\sin(q_x x) + \theta_T(z)\cos(q_x x)$$

with similar expressions for the other two perturbations. Clearly, θ_U and θ_T will have opposite symmetry. If θ_U, ϕ_U and ψ_U have the symmetry of SOLUTION 1, then θ_T, ϕ_T and ψ_T will possess the symmetry of SOLUTION 2. Substituion in (6)–(8) yields six coupled ordinary differential equations for the six functions ψ_U, ψ_T, etc. From (10), six boundary conditions also result which are qualitatively identical to those of HD. Without loss of generality, one can use the *ansatz* in which ϕ_U, ψ_T, θ_U are even and ϕ_T, ψ_U, θ_T odd with respect to the sample centre. An *ansatz* with opposite parity results from the first by shifting the origin through a quarter of a wavelength of periodicity along x axis. As the sample has effectively infinite extent along x, the threshold will remain unchanged under this transformation. With a sufficiently high stabilizing electric strength E_{xo}, (6)–(10) are solved by the series solution method and the critical magnetic strenth $H_\perp = H_J(Q_x)$ obtained as a function of the dimensionless wavevector $Q_x = q_x h$ for given values of the magnetic and director tilts. When Q_x is small, $H_J(Q_x) \to H_F$ of (12). The resulting neutral stability curve has a minimum $H_{PX} = H_J(Q_{PX})$ at $Q_x = Q_{PX}$. Then, H_{PX} is taken as the xz Mode

threshold and Q_{PX} as the wavevector of periodicity at threshold . The ratio

$$r_X = H_{PX} / H_F$$

as well as Q_{PX} can be studied as functions of different parameters. As long as $r_X < 1$, the xz Mode has lower threshold than HD and is more favourable than HD. When $r_X \geqslant 1$, HD is more favourable than the xz Mode. As the boundary conditions for the xz Mode and HD are the same, $Q_{PX} \to 0$ when $r_X \to 1$, in general. Regarding Q_{PX} as the order parameter, the transition from uniform alignment $\mathbf{n}_0$ to PD with x modulation can be said to be one of second order. An obvious effect of the increase of director pretilt away from the homeotropic is to increase the the xz Mode threshold with respect to the HD threshold at given values of magnetic tilt and stabilizing voltage.

The solution for the yz Mode threshold is effected in a similar way by the computation of corresponding quantities

$$r_Y = H_{PY} / H_F$$

and Q_{PY}. But in this case, the boundary conditions for PD are not identical to those of HD. While the vanishing of perturbations θ and ϕ at the boundaries remains common, the restriction on ψ is different from that for HD (note the term $-\varepsilon_A S C \psi_{,y}$ in eqn. 10). Hence, when $r_Y \to 1$, Q_{PY} may not vanish in general. Regarding Q_{PY} as the order parameter, the transition from the uniform alignment to the yz Mode PD will be one of first order.

The procedure for solution of the xyz Mode is identical to that used for the xz and yz Modes except that the periodicity is determined by sin $[q(C_\mu x + S_\mu y)]$ and cos $[q(C_\mu x + S_\mu y)]$ where q is the amplitude of the wavevector and μ the angle between the wavevector and x axis. The boundary conditions (10) yield the critical magnetic field as a function of the reduced wavevector $Q = q h$ and μ: $H_J(Q, \mu)$; this defines a neutral stability surface. For suitable values of parameters, the surface exhibits a minimum at $H_J(Q_P, \mu_P)$ and this is regarded as the xyz Mode threshold. Results are not presented for the xyz Mode as its threshold is generally higher than those of the xz and yz Modes. Thus, xz and yz Modes become the only relevant instability modes (as for homeotropic alignment).

Calculations are performed for the parameters of $M1$ [19] at a reduced temperature of 0.9:

$$(K_1, K_2, K_3) = (16.1, 5.2, 18.3)10^{-7}\, dyne;\ \chi_A = 1.39\ 10^{-7}\, emu;$$

$$\varepsilon_\parallel = 8.9; \varepsilon_\perp = 22.8; \varepsilon_A = -13.9. \qquad (14)$$

The strength of the stabilizing $\mathbf{E}_0$ is expressed in terms of the reduced field $R_E = E_{xo}/E_M$ with E_M being defined as (see eq. 18 of ref. 21)

$$E_M{}^2 = \frac{\pi^3 K_1 \varepsilon_\parallel{}^2}{\varepsilon_\perp \varepsilon_A{}^2 h^2}. \tag{15}$$

Figure 1 contains plots of r_X, r_Y and Q_{PX}, Q_{PY} as functions of R_E for different values of magnetic tilt α and director pretilt ϕ_o. When α is small ($\mathbf{H}_\perp$ almost parallel to x axis; Figs. 1a, 1b), the yz Mode is more favourable than the xz Mode over almost the entire range of R_E. When R_E attains low values, $r_X \to 1$ and $Q_{PX} \to 0$. The yz Mode exists as a solution in this R_E range, but it is of no real interest as $r_Y > 1$. This serves to highlight the contrast between the xz and yz Modes which is mainly due to the different boundary conditions obeyed by them.

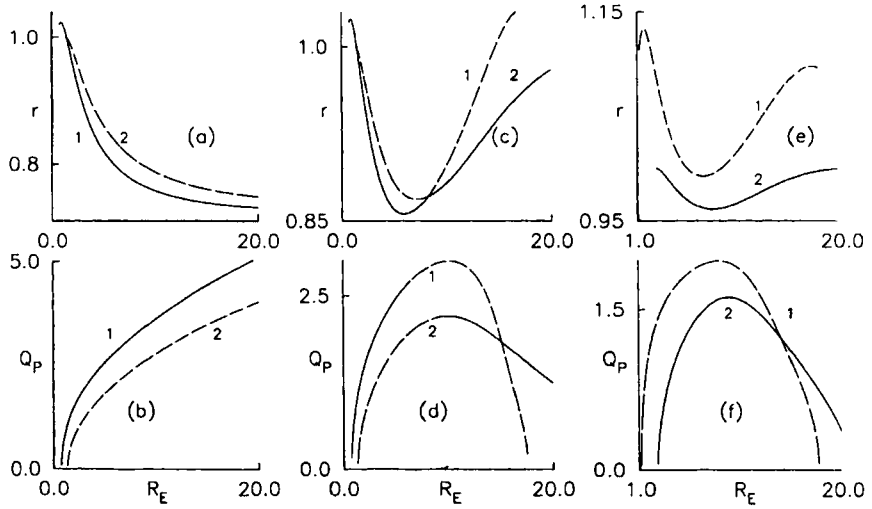

FIGURE 1 Intitial uniform orientation of the nematic director in the yz plane making angle ϕ_o with z axis. Material parameters are those of $M1$ (14) so that $\mathbf{H}_\perp$ (3) destabilizes the orientation while $\mathbf{E}_0$ (applied along x) stabilizes it; α is the tilt of $\mathbf{H}_\perp$ away from $\mathbf{E}_0$. The yz and xz Modes are periodic deformations with periodicity along y and x, respectively. $r_Y = H_{PY}/H_F$ and Q_{PY} are the reduced yz Mode threshold and dimensionless wavevector of periodicity at threshold, respectively, where H_F is the threshold for the aperiodic or homogeneous distortion (12); r_X and Q_{PX} describe corresponding quantities for the xz Mode. Plots of r_X, r_Y and Q_{PX}, Q_{PY} as functions of the reduced electric field $R_E = E_{xo}/E_M$ (see equation 15). The diagrams are drawn for α = (a,b) 0.01; (c,d) 0.1; (e,f) 0.1 radian and ϕ_o = (a,b) 0.4; (c,d) 0.4; (e,f) 0.8 radian. Curves 1,2 correspond to the yz Mode and the xz Mode, respectively. The dashed lines indicate portions of curves which are of no real interest (see section 3.2).

The nature of variation of r and Q_P changes drastically when α is increased ($\mathbf{H}_\perp$ is tilted away from the x axis; Figs. 1c–1f). Both the xz and the yz Modes have limited R_E ranges of existence; thus, a sufficiently strong stabilizing $\mathbf{E}_0$ can quench both the PD Modes. This result is qualitatively similar to that found for homeotropic alignment (see Fig. 2 of ref. 21). For a given Mode, its R_E range of existence becomes narrower when the director pretilt is increased (compare Figs. 1c,1d with 1e,1f). For a given value of ϕ_o, the xz Mode has a wider R_E range than the yz Mode. Over the R_E range where the yz Mode is more favourable than the xz Mode, $Q_{PY} > Q_{PX}$; hence, the yz stripes are narrower than the xz stripes (see, Fig. 1d). A transition between the two PD Modes (Figs. 1c,1d) should be accompanied by a discontinuous change in the wavevector. When ϕ_o is sufficiently high (Figs. 1e, 1f), the yz Mode exists as a solution of the governing equations but appears to be totally unfavourable over the entire R_E range.

The variations of r and Q_P with the magnetic tilt α (Fig. 2) at different director tilts ϕ_o and reduced stabilizing electric fields R_E complements the results of Figure 1. In general, the yz Mode is more favourable than the xz Mode only when $\mathbf{H}_\perp$ is aligned sufficiently close to x axis. As α is increased, both PD Mode thresholds increase, but the xz Mode becomes more favour-

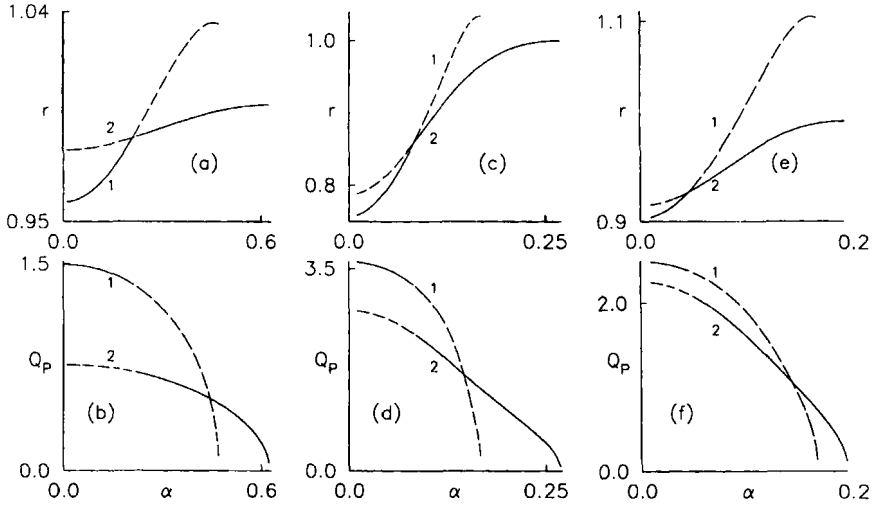

FIGURE 2 r_X, r_Y and Q_{PX}, Q_{PY} as functions of the magnetic tilt α for $M1$ with relevant details common to Figure 1. The reduced electric strength R_E = (a,b) 2; (c,d) 10; (e,f) 10. The director pretilt at the boundaries is ϕ_o = (a,b) 0.4; (c,d) 0.4; (e,f) 0.8; see section 3.

able than the *yz* Mode. A crossover occurring between the two PD Modes with α variation should be again accompanied by a discontinuous change in the wavevector. Increase of ϕ_o at a given R_E reduces the α range of existence of both PD Modes (Figs. 2c–2f). At a given ϕ_o, the α range of existence of either PD Mode is wider at $R_E = 2$ (Figs. 2a, 2b) than at a higher value of R_E (= 10; Figs. 2c, 2d). This is not only reminiscent of similar results obtained for the homeotropic orientation (see Fig. 3 of ref. 21) but also indicative of the shapes of the phase boundaries separating the PD Modes and HD in the $R_E - \alpha$ plane.

Figure 3 depicts plots or r and Q_P with the director pretilt ϕ_o at different values of the magnetic tilt, α and reduced electric strength R_E. This variation is being studied only from the theoretical view point because ϕ_o is a parameter that enters the equations; obviously, this is not experimentally feasible as it is not convenient to vary the director pretilt in small increments. The conclusions of the previous diagrams are supported by Fig. 3. Increase of ϕ_o away from the homeotropic has a deleterious effect on the formation of PD (increase of PD threshold relative to the HD threshold and diminution of wavevector). A given PD Mode can be quenched when ϕ_o is increased beyond a certain limit. At a given R_E, the ϕ_o range of existence of

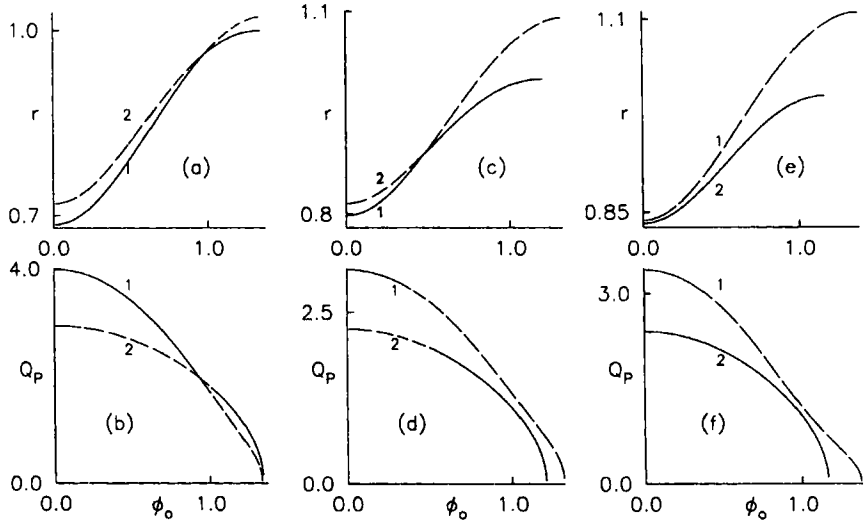

FIGURE 3 Plots of r_X, r_Y and Q_{PX}, Q_{PY} versus the director pretilt angle ϕ_o for different magnetic tilts α and reduced electric strengths R_E; the material is $M1$. For definitions, see the caption of Figure 1. The diagrms are drawn for α = (a,b) 0.01; (c,d) 0.1; (e,f) 0.1. R_E = (a,b) 10; (c,d) 5; (e,f) 10; see section 3.

a given PD Mode shrinks when α is increased (compare Figs. 3a, 3b with Figs. 3e, 3f). In general, the ϕ_o range of existence of the xz Mode is broader than that of the yz Mode. In particular when α and R_E are sufficiently high (Figs. 3e, 3f), the yz Mode appears to be of no interest over the entire range of ϕ_o.

For homeotropic orientation [21], the technique of ref. 24 can be employed to obtain analytical expressions for phase boundaries because of two reasons. Firstly, only SOLUTION 1 is relevant in ref. 21. Secondly, the boundary conditions for the PD Modes and HD are identical so that the given *PD* Mode merges into HD in the limit of vanishing wavevector. As both these attributes are lacking in the solutions studied here, the technique of ref. 24 cannot be used. The only alternative is to obtain the critical boundaries numerically.

For the critical boundary in the $R_E - \alpha$ plane, for instance, ϕ_o is held fixed at some value. R_E is given a sufficiently large value (say, 10). Starting from a low value, say, $\alpha = 0.01$ radian, α is increased and the yz Mode threshold studied as a function of α. At some $\alpha = \alpha_M$, the yz threshold becomes equal to the HD threshold ($r_Y = 1$); generally, at this value of α, $Q_{PY} \neq 0$. By diminishing R_E in suitable steps and plotting R_E versus α_M, the critical boundary for the yz Mode can be plotted. The procedure is repeated for the xz Mode. In this case, the limits $r_X \to 1$ and $Q_{PX} \to 0$ generally occur at the same α_M for a given R_E. An analogous procedure is adopted to compute the critical boundaries of the PD Modes in the $R_E - \phi_o$ plane when the magnetic tilt is kept fixed at some value.

Figures 4a–4d contain the numerically determined critical boundaries of the PD Modes and capture the essential features of the relative stability of the two PD Modes (compare with Figs. 1–3). The yz Mode has narrower α and R_E ranges of existence than those of the xz Mode; both the R_E and the α ranges of occurrence of a given PD Mode shrink when the director pretilt is enhanced (Figs. 4a, 4b). The relative positions of the critical boundaries (especially in the low R_E range) are worth noting due to a slight difference between Figures 4a, 4b and Figure 1 of ref. 21. The regions marked XZ and HD correspond uniquely to the regions of existence of these two deformations. The region of existence of the yz Mode is contained within that of the xz Mode. Hence, the inner region is labeled by both XZ and YZ as both PD Modes exist as solutions. At a given (R_E, α) in this overlap region, either the yz Mode or the xz Mode is considered the more favourable Mode depending upon which Mode has the lower threshold.

Similar conclusions can be reached by studying Figures 4c, 4d though the shapes of the critical boundaries are found to be somewhat different from

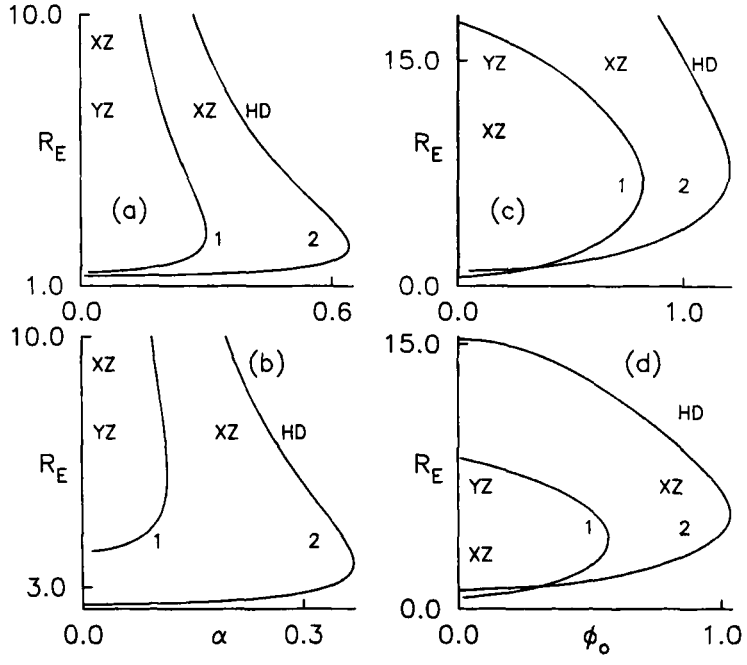

FIGURE 4 Critical boundaries of the *yz* (curves 1) and the *xz* (curves 2) Modes for *M*1. Figures 4a, 4b depict the phase diagrams in the R_E-α plane for director pretilt angles ϕ_o = (a) 0.4; (b) 0.8 radian. Similarly, Figures 4c, 4d contain the critical boundaries drawn in the R_E-ϕ_o plane for the magnetic tilt α = (c) 0.1; (d) 0.2 radian. The phase boundary for a given PD Mode (determined numerically) is the locus of points at which the PD Mode threshold equals the HD threshold. At these points, the wavevector of periodicity of the given PD Mode need not necessarily vanish. As explained in section 3, these diagrms reflect the essential features of the PD Modes summarized in figures 1-3; (see section 3).

those given in Figures 4a, 4b. The *xz* Mode has broader ϕ_o and R_E ranges of existence than those of the *yz* Mode. The ϕ_o and the R_E ranges of occurrence of either PD Mode shrink with an increase in the magnetic tilt, α. Remarks made about Figures 4a, 4b also hold here except that there exists a small triangular portion near the origin where only the *yz* Mode can occur; this region has not been labeled with YZ due to paucity of space.

4. MATERIALS WITH $\varepsilon_A > 0, \chi_A > 0$

It seems meaningful to compare results of the previous section with those for a material such as 5CB [25]. In this case, the destabilizing $\mathbf{E}_0$ acts along

x and the stabilizing $\mathbf{H}_\parallel$ is applied along $\mathbf{n}_0$; in this section, we put $H_\perp = 0$. For dependence of perturbations on z, ϕ gets decoupled from θ and ψ and damps out. Using an *ansatz* similar to that employed in section 2, the HD electric threshold E_F can be calculated by solving (6),(7) and (10):

$$E_F{}^2 = \frac{4\pi\omega_3\omega_4}{\varepsilon_A\varepsilon_\perp h^2}\left(\frac{\pi^2}{4} + \frac{\chi_A h^2 H_\parallel{}^2}{\omega_4}\right) \tag{16}$$

Results obtained earlier[18] for the homeotropic orientation are briefly summarized; the reasoning is similar to that employed in section 3.1.

4.1. Results for $\phi_o = 0$

With $\mathbf{n}_0$ along z, HD is described by $\theta(z)$ and $\psi(z)$. As E'_z stabilizes $\mathbf{n}_0$, the HD threshold (16) is scaled up by the factor $\sqrt{\varepsilon_\parallel/\varepsilon_\perp}$. For the xz Mode , θ and ψ are periodic along x and are in phase with a variation of $\sin(q_x x)$, say. As there is variation with x and z, E′ has both x and z components related by Maxwell's curl equation, $E'_{x,z} = E'_{z,x}$. Of these, E'_z is in phase with θ along x, has the same symmetry as θ and produces a stabilizing influence on the director; E'_x is antisymmetric with respect to the sample centre, is out of phase with respect to θ along x but has a destabilizing influence on $\mathbf{n}_0$. The *ansatz* for perturbations is such that θ is even and ψ odd relative to the sample centre (the symmetry is that of SOLUTION 1 of section 3.1); we ignore the other uncoupled solution with opposite spatial symmetry. Due to the additional destabilizing influence not found in HD, the xz Mode threshold may become lower than the HD threshold under conditions which become evident from the neutral stability curve described by,

$$E_{xo}{}^2 = \frac{\beta Q_x^4 + \gamma Q_x^2 + \delta}{\zeta(Q_x{}^2 + \frac{\pi^2}{4})};\ \zeta = \frac{\varepsilon_\perp\varepsilon_A h^2}{4\pi K_3\varepsilon_\parallel};\ \beta = \frac{K_1\varepsilon_\perp}{K_3\varepsilon_\parallel};$$

$$Q_x = q_x h;\ \gamma = \frac{\chi_A\varepsilon_\perp h^2 H_\parallel{}^2}{K_3\varepsilon_\parallel} + \frac{\pi^2}{4}\left[\frac{\varepsilon_\perp}{\varepsilon_\parallel} + \frac{K_1}{K_3}\right];$$

$$\delta = \frac{\pi^2}{4}\left[\frac{\pi^2}{4} + \frac{\chi_A h^2 H_\parallel{}^2}{K_3}\right]. \tag{17}$$

By extremizing this expression with respect to Q_x, the xz Mode threshold $E_{PX} = E_{xo}(Q_{PX})$ may be found. For small wavevectors, (17) becomes,

$$E_{xo}{}^2 \approx E_F{}^2\left[1 - Q_x{}^2\left(\frac{4}{\pi^2} - \frac{\gamma}{\delta}\right)\right].$$

The xz Mode threshold will be less than the HD thershold if $H_\parallel > H_C$ with

$$H_C{}^2 = \frac{\pi^2[K_3\varepsilon_\perp + (K_1 - K_3)\varepsilon_\parallel]}{4\chi_A\varepsilon_A h^2}. \tag{18}$$

A reduced stabilizing magnetic strength can now be defined as

$$r_H = H_\parallel / H_C.$$

The reduced xz Mode threshold is defined as

$$R_X = E_{PX}/E_F$$

with E_F given by (16). For $r_H > 1$, $R_X < 1$. Increase of $H_\parallel$ diminishes R_X and increases Q_{PX}(the stripes become narrower). In the limit of $r_H \to 1$, $R_X \to 1$ and $Q_{PX} \to 0$ showing that H_C of (18) defines a critical point separating HD and the xz Mode.

Results for the yz Mode are described in an analogous manner except that the reduced threshold is now

$$R_Y = E_{PY}/E_F$$

and the dimensionless wavevector is denoted by Q_{PY}. An important difference between the yz and xz Modes arises when K_2 is sufficiently smaller than K_1. Even in the limit of $r_H \to 0$, the yz Mode exists with a small but non-zero wavevector (domains are wide) and R_Y remains less than unity (mathematically, the critical point defined in (18) is imaginary when K_2 replaces K_1). With increase of r_H, R_Y diminishes further and Q_{PY} increases but the yz Mode threshold remains less than the xz Mode threshold for all stabilizing $H_\parallel$. Hence, in a material such as 5CB neither HD nor the xz Mode is favourable; only the yz Mode should be observable. The results presented for the xz Mode are of theoretical interest and only serve for

comparison. In a way this is predictable because the twist elastic constant, K_2, is less than the splay constant, K_1.

4.2. Results for $\phi_o \neq 0$

With the above recapitulation, it is easier to understand what to expect when $\mathbf{n}_0$ deviates from the homeotropic alignment. The three PD Modes that can be studied are–the xz, the yz and the xyz. The nature of the perturbations for the PD Modes should be carefully noted because of the qualitative change in the magnetic coupling as compared to that in section 3 (see eqns. 7 to 9).

The xz Mode can exist as one of two decoupled solutions each of which is associated with perturbations with definite spatial symmetry relative to the sample centre:

Solution A: θ is even; ϕ and ψ are odd
Solution B: θ is odd; ϕ and ψ are even.

Solution A is found to have lower threshold than Solution B. The symmetries of θ and ψ associated with Solution A are the same as those of HD. Additionally, the xz Mode and HD have the same set of boundary conditions for θ and ψ. Hence, the threshold for Solution A will tend to E_F (16) in the limit of vanishing wavevector. When $\mathbf{n}_0$ is tilted away from the homeotropic, the xz Mode threshold increases because of the additional (antisymmetric) perturbation ϕ. This adds to the elastic free energy (equivalently, a higher elastic stabilizing torque is to be overcome by the destabilizing torques) but does not bring in additional destabilizing influence (ϕ does not perturb the electric field).

When ϕ_o is increased from zero, the yz Mode threshold will also increase with respect to that for the homeotropic case, but the cause is somewhat different. In this case, ϕ gets decoupled from θ and ψ. As ϕ has no direct coupling with $\mathbf{E}_0$, it damps out. In principle, this decoupling should diminish the yz Mode threshold as the elastic deformation energy associated with ϕ is removed. What actually happens is the reverse because the governing equations (6) and (7) do not support solutions with pure spatial symmetry. For θ and ψ, solutions are of the form given in section 3.2; for instance,

$$\theta(y,z) = \theta_U(z)\sin(q_y y) + \theta_T(z)\cos(q_y y).$$

Effectively, the addition of terms with opposite spatial symmetry increases the elastic free energy and also diminishes the destabilizing contribution arising from electric field modifications. Additionally, the boundary

condition on ψ (10) for the yz Mode is different from that for HD. Hence, the yz Mode threshold equals E_F (16) at nonzero wavevector of periodicity and a continuous transition between the yz Mode and HD is ruled out.

The xyz Mode can be studied exactly as in section 3. Each perturbation is written as the sum of two parts having opposite spatial symmetry relative to the sample centre. The threshold is found from the minimum of a neutral stability surface defined by the dependence of E_{xo} on Q and μ where Q is the dimensionless wavevector amplitude and μ the inclination of the wavevector with x axis. For strong stabilizing $\mathbf{H}_1$ (high r_H), this minimum occurs at $\mu = \pi/2$ and the threshold coincides with the yz Mode threshold. In the low r_H range, the xyz Mode threshold corresponds to the xz Mode threshold with $\mu = 0$. There exists no other point in the range $0 < \mu < \pi/2$ at which the neutral stability surface exhibits a minimum regardless of the magnitude of r_H. This is, perhaps, a consequence of $\mathbf{H}_1$ acting along $\mathbf{n}_0$ and not breaking the cylindrical symmetry about $\mathbf{n}_0$. The xyz Mode is, therefore, not studied.

Having argued that the threshold for a given Mode (xz or yz) will increase with director pretilt, it is necessary to compare them. This is essential because when ϕ_o is zero the xz Mode is of no real interest [18] (as already explained in section 4.1). With a change in the structure of both the Modes produced by initial director pretilt, it should be interesting to investigate whether the xz Mode will now become observable. Results for 5CB are obtained with material parameters [25] at 28°C:

$$(K_1, K_2, K_3) = (5.21, 2.71, 6.67)\,10^{-7}\ dyne;\ \chi_A = 1.1\,10^{-7}\ emu;$$

$$\varepsilon_\parallel = 17.86;\ \varepsilon_\perp = 7.25;\ \varepsilon_A = 10.61. \tag{19}$$

The reduced thresholds R_X and R_Y as well as the corresponding periodicity wavevectors Q_{PX} and Q_{PY} are determined from the minima of the respective neutral stability curves from a series solution of the governing equations. These quantities can now be studied as functions of different parameters.

Figure 5 contains plots of R and Q_P as functions of r_H the reduced stabilizing magnetic strength for different ϕ_o. When $\mathbf{n}_0$ is close to the homeotropic (Figs. 5a, 5b), the yz Mode is favourable over the entire range of r_H; results for the xz Mode have been included only for comparison. When the director pretilt is high enough (Figs. 5c, 5d), the xz Mode should be observable for low r_H. Though the yz Mode persists all the way down to $r_H = 0$, it is of no real interest as its threshold is higher than the xz Mode and HD thresholds. The direction of periodicity should switch from y to x when r_H is

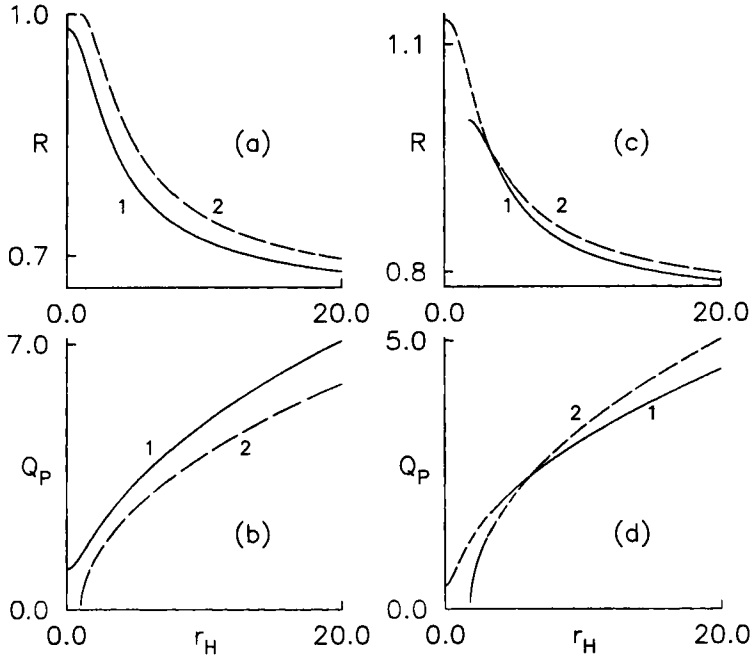

FIGURE 5 Initial uniform director alignment, $\mathbf{n}_0$, is in the yz plane making angle ϕ_0 with z axis. The material chosen is 5CB with material parameters (19). $\mathbf{H}_1$, applied along $\mathbf{n}_0$, stabilizes the initial orientation while $\mathbf{E}_0$, impressed along x axis, serves as the destabilizing influence. The reduced magnetic strength $r_H = H_1/H_C$ where H_C is defined in (18). The reduced PD threshold for the yz Mode is $R_Y = E_{PY}/E_F$ where E_F is the threshold for the aperiodic mode (16). Similar definitions hold for the xz Mode. The dimensionless wavevectors at threshold, Q_{PX}, Q_{PY} of the xz and yz Modes and their respective reduced threshold R_X, R_Y are plotted as function of r_H. The director pretilt angle $\phi_o = (a,b)\ 0.01$; (c,d) 0.75. Curves 1 and 2 drawn, respectively, for the yz and the xz Modes; (see section 4.2).

diminished; this should also be accompanied by a discontinuous change in the stripe width. The xz Mode has a cut off in the low r_H region below which only HD should appear. This cut off increases with ϕ_o; as the director pretilt is increased, the r_H range of existence of HD should widen.

The variation of R and Q_P with ϕ_o *at different* r_H (Fig. 6) supports the conclusions of Figure 5. The yz Mode should be observable when the director pretilt is close to the homeotropic. When ϕ_o is high enough, the xz Mode threshold can become less than that of the yz Mode. If this occurs then it should also be accompanied by a discontinuous change in the wavevector. The ϕ_o range of existence of both Modes shrinks when r_H is lowered (compare Figs. 6ab with Figs. 6cd). But the range of existence of the xz Mode broadens with respect to that of the yz Mode.

The phase boundaries for the xz and yz Modes are shown in Figure 7 for 5CB parameters. These are determined numerically as described in the previous section. The wavevector of the xz Mode tends to zero when the xz Mode threshold approaches the HD threshold (curve 2). This is not true, in general for the yz Mode; the yz Mode boundary (curve 1) corresponds to the yz Mode threshold equalling the HD threshold, but the wavevector may not be zero. When the director pretilt is close to the planar, only HD can exist regardless of the stabilizing r_H (the region marked HD). When r_H is high enough and ϕ_o sufficiently elevated, the xz Mode should be more favourable than the yz Mode (this is the region marked XZ); however, the xz Mode has a lower cutoff and is unfavourable when r_H and ϕ_o are close to zero. In this region, the yz Mode prevails (region marked YZ). In the overlap region, the thresholds for both PD Modes have to be computed and the Mode with lower threshold assumed to exist.

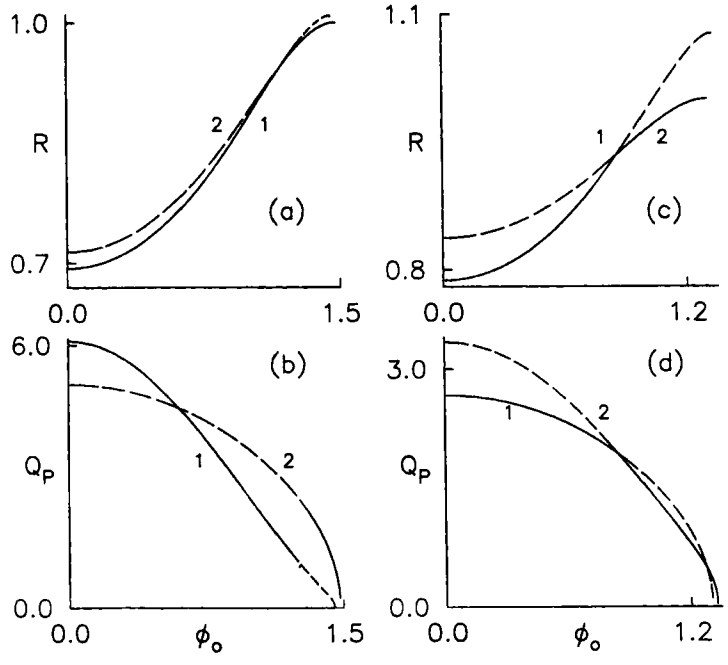

FIGURE 6 Variation of reduced electric thresholds, R_X,R_Y and dimensionless wavevectors Q_{PX}, Q_{PY} as functions of the director pretilt angle, ϕ_o for different values of reduced stabilizing magnetic strength, r_H; relevant details as in Figure 5. r_H = (a,b) 15; (c,d) 5. Curves 1 and 2 are drawn, respectively, for the yz and the xz Modes; (see section 4.2).

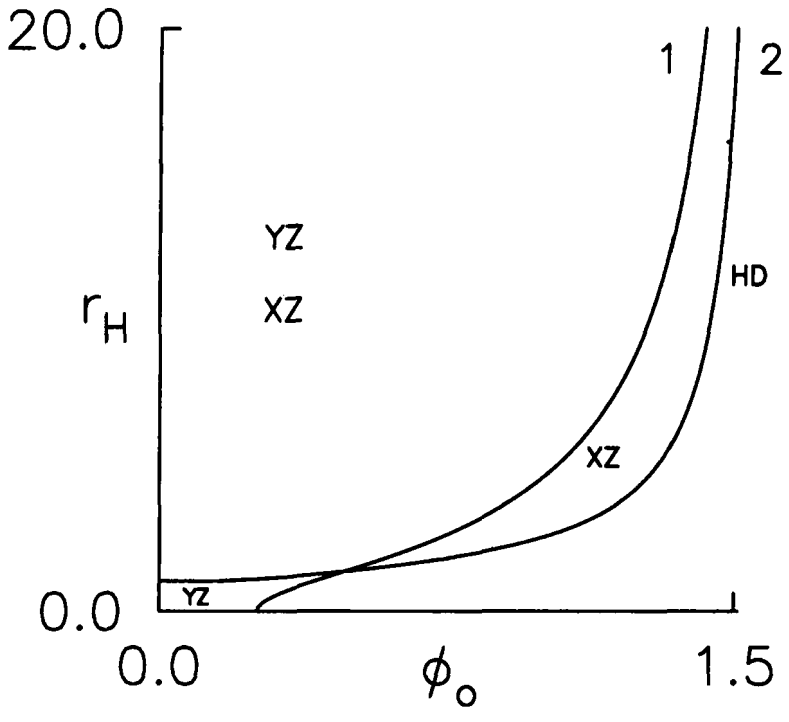

FIGURE 7 Phase boundaries for the xz and yz Modes in the r_H-ϕ_o plane for 5CB (19); definitions are as in Figure 5. The conclusions of Figures 5 and 6 are supported (section 4).

Some of the results can be understood qualitatively. A basic difference between the two PD Modes is their structure. The xz Mode is associated with perturbations having pure spatial symmetry and can evolve continuously out of HD. The yz Mode is a mixture of two components of opposite spatial symmetry which get decoupled for homeotropic orientation with one of them having higher free energy than the other. One can now appreciate why the yz Mode threshold should exceed that of the xz Mode when ϕ_o increases. For general values of ϕ_o, the principal stabilizing torques associated with x periodicity are $K_1\theta_{,xx}$ and $K_2\phi_{,xx}$(equations 7 and 8). On the other hand, the corresponding torque for the yz Mode is $(K_2C^2 + K_3S^2)\theta_{,yy}$(equation 7). When ϕ_o is increased from 0 to $\pi/2$, the effective elastic constant increases more than two fold from K_2 to K_3. Hence, the yz Mode threshold can be expected to increase more rapidly than the xz Mode threshold when ϕ_o is varied from zero. The mixing of Solutions A and B in determining the yz Mode appears to only add to this effect.

5. CONCLUSIONS, LIMITATIONS OF MATHEMATICAL MODEL

The linear perturbation model of earlier work [18, 21] has been extended to study the effect of director pretilt on the occurrence of static periodic deformations produced by the application of **E** and **H** fields in two materials (*M*1 and 5CB) having positive diamagnetic anisotropy and dielectric anisotropies of opposite sign. The rigid anchoring hypothesis is used. Qualitative explanations for the occurrence or non-occurrence of PD are given in different parts of the text by comparing the present solutions with those obtained (for initial homeotropic alignment) in the absence of pretilt. The main conclusions are as follows.

In *M*1 (section 3), results are similar to those obtained earlier [21] for the homeotropic alignment when the director pretilt (ϕ_o) away from the homeotropic is small. When the stabilizing $\mathbf{E}_0$ is weak enough, only HD occurs under the action of a destabilizing $\mathbf{H}_\perp$. For sufficiently strong $\mathbf{E}_0$, *PD* results over a range of magnetic tilt α; a variation of α (at fixed $H_\perp$) or of $H_\perp$ (at given α) leads to discontinuous change of wavevector. *PD* is suppressed and only HD results if $\mathbf{H}_\perp$ is impressed sufficiently away from $\mathbf{E}_0$. The new results of this work pertain to a variation of ϕ_o and show that PD can be quenched if the director pretilt is far away from the homeotropic; in particular, *PD* governed by (6)–(10) should not occur for planar alignment ($\phi_o = \pi/2$). Phase boundaries for different PD Modes are presented.

Results for 5CB are an extension of those of an earlier work [18]. For homeotropic alignment, PD sets in if the stabilizing $\mathbf{H}_\parallel$ is strong enough with wavevector normal to $\mathbf{E}_0$. When the director pretilt is high enough, *PD* with wavevector along $\mathbf{E}_0$ is more favourable. Beyond a limiting ϕ_o and also for weak $\mathbf{H}_\parallel$, PD cannot exist; only HD occurs. The phase boundaries for different deformations are given.

The limitations of the mathematical model used as well as possible experiments for homeotropic alignment have been discussed in detail (section 5, ref. 21). A few relevant points are discussed here. The linear perturbation analysis results in an eigenvalue problem whose solution does not lead to the complete determination of the amplitudes of perturbations; hence, possible nonlinear effects occurring above threshold cannot be readily predicted. Taking into account previous results, the following possibilities connected with post threshold distortions may be noted.

(i) In an experiment, a deformation is deteched above threshold only when it becomes nonlinear. The measured wavevector of PD above threshold may not agree with the value calculated at threshold by the linear

analysis. It is also clear that when the destabilizing field is increased above PD threshold, the periodicity should also change; this again falls outside the scope of a linear theory.

(ii) Another aspect of nonlinearity is the effect of increasing the destabilizing field well above PD threshold; this can be illustrated with an example. Consider $M1$. As this material has $\chi_A > 0$, the director in a sample will tend to align along $\mathbf{H}_\perp$ when $H_\perp$ is high enough; in such a case, there can be no periodicity of distortion. Suppose PD is observed in a sample of $M1$ under the joint action of $\mathbf{E}_0$ and $\mathbf{H}_\perp$. As pointed out in (i), increase of $H_\perp$ above PD threshold should affect the periodicity of distortion. With the initial remarks in (ii), it is clear that the wavevector should diminish with increase of $H_\perp$. Finally, periodicity should disappear when $H_\perp$ attains some high value. Such an effect has been predicted an detected experimentally in a different situation [5]. The arguments for $M1$ can be repeated for 5CB except that PD is induced with a stabilizing $\mathbf{H}_\parallel$ and a destabilizing $\mathbf{E}_0$. A linear calculation cannot shed light on such possibilites.

(iii) For definiteness, consider $M1$. The linear analysis shows that if $\mathbf{H}_\perp$ is impressed sufficiently away from $\mathbf{E}_0$, PD cannot set in. Above a threshold, HD appears. When $H_\perp$ is increased above HD threshold, the amplitude of HD will appreciate. This will cause considerable modification of $\mathbf{E}$ inside the sample. The possibility cannot be ruled out that when HD develops above threshold it may become unstable against periodic perturbations to result in PD. The situation is similar to that of a nematic sample in the vicinity of the smectic A-nematic transition temperature exhibiting a striped distortion when subjected to a magnetic field [6]. The analysis in such a case will have to be carried out along the lines of Allender *et al.* [12]. Clearly, the linear perturbation model of the present work is insufficient to study such deformations. From point (ii), one can conclude that even if PD appears in such a situation, it will get quenched when the destabilizing $\mathbf{H}_\perp$ becomes strong enough.

(iv) In the present work, $\phi_o = \pi/2$ refers to planar alignment with $\mathbf{n}_0$ in the yz plane. In the linear approximation, PD is found not to occur in this configuration. It is also possible to study planar alignment with $\mathbf{n}_0$ along x. In a material such as 5CB, $\mathbf{E}_0$ stabilizes $\mathbf{n}_0$. One can now study the effects of a destabilizing $\mathbf{H}$ applied in the yz plane. A linear analysis shows that PD of different kinds may set in; these results will be presented separately [26].

Effects of material parameter variation have not been presented. The values of material parameters may have an important bearing on the phase boundaries separating different deformations and hence on the shape of phase diagrams presented in this work. If a given experiments is performed at different temperatures, this study becomes necessary as material parameters are known to vary with temperature. The anchoring is assumed to be rigid. It is found [26] that the nature of the transition between PD and HD may be affected when the anchoring is not strong [10]. In practice, the variation of ϕ_o cannot be effected continuously; for each pretilt, a different surface treatment may be needed and this may mean a different surface free energy. The assumption of rigid anchoring prevents the need to include some of these relevant parameters in a preliminary analysis.

Flexoelectricity [9] is ignored. Hence, results for *dc* fields may be quite different [27] if deformations set in without threshold. Similarly, surface elastic constants have been left out. This assumption may not be unrealistic for sufficiently thick samples. The nematic is assumed to be an insulator. In samples with ionic impurities, the possibility of electrohydrodynamic convection cannot be ruled out (see ref. 28 for reviews). In case the positive feedback mechanism for convection [28] does not exist, it may still be possible to experimentally check the conclusions of this work.

All boundary conditions deduced from the electromagnetic theory cannot be imposed on **E** [23]. In an actual experiment, the electrodes cannot be placed too far apart as the voltage necessary to produce instability becomes very high. When the electrode gap is not much larger than the sample thickness, boundary conditions may have to be imposed at the electrodes. Then, the harmonic dependence of perturbations on x and y will not suffice in a theoretical treatment. The present model assumes that the ground state $\mathbf{n}_0$ remains undeformed upto threshold. Experiments indicate [29] that this assumption may not be valid when the electrodes do not have a flat surface. It appears [30] that even with flat electrodes, the ground state may get distored before suffering instability.

It must be remembered that only two kinds of material are studied. Results for a material such as CCH-7 [20] are not included. In such a material, the xyz Mode PD sets in even in the absence of a stabilizing $\mathbf{H}_\perp$ when the alignment is homeotropic [21]; the wavevector also changes continuously with magnetic tilt. It is found [26] that PD in CCH-7 can be quenched by increasing the director pretilt. The results are, however, somewhat involved as PD may go over from the xyz Mode to HD via the xz Mode or via the yz Mode depending upon α and ϕ_o; these results will be separately communicated [26].

Acknowledgement

The author thanks a Referee for useful comments which helped imporve an earlier version of the manuscript.

References

[1] P. G. de Gennes and J. Prost, *The Physics of Liquid Crystals*, (Clarendon Press, Oxford, 1993).
[2] S. Chandrasekhar, *Liquid Crystals*, (Cambridge University Press, 1992).
[3] L. M. Blinov and V. G. Chigrinov, *Electrooptic Effects in Liquid Crystal Materials*, (Springer Verlag, 1993).
[4] S. A. Pikin, *Structural Transformations in Liquid Crystals*, (Gordon and Breach, 1991).
[5] F. Lonberg and R. B. Meyer, *Phys. Rev. Lett.*, **55**, 718 (1985), G. Srajer, F. Lonberg and R. B. Meyer, *Phys. Rev. Lett.*, **67**, 1102 (1991).
[6] C. Gooden, R. Mahmood, A. Brisbin, A. Baldwin, D. L. Johnson and M. E. Neubert, *Phys. Rev. Lett.*, **54**, 1035 (1985).
[7] L. K. Vistin, *Sov. Phys. Crystallogr.*, **15**, 514 (1970).
[8] W. H. De Jeu, C. J. Gerritsma, P. Van Zanten and W. J. A. Goossens, *Phys. Lett.*, **39 A**, 335 (1972).
[9] R. B. Meyer, *Phys. Rev. Lett.*, **22**, 918 (1968), J. Prost and J. P. Marcerou, *J. Phys. France*, **38**, 315 (1977), G. Durand, *Mol. Cryst. Liquid Cryst.*, **113**, 237 (1984).
[10] A. Rapini and M. Papoular, *J. Phys. Colloq. France*, **30**, C4–54 (1969), for reviews on interfacial properties, see J. Cognard, *Mol. Cryst. Liquid Cryst. Suppl.*, **1**, 1 (1982) and B. Jerome, *Rep. Progr. Phys.*, **54**, 391 (1991).
[11] H. J. Deuling, *Solid State Physics Supplement*, **14**, 77 (1978).
[12] Yu. P. Bobylev, V. G. Chigrinov and S. A. Pikin, *J. Phys. Colloq. France*, **40**, C3-331 (1979), U. D. Kini, *J. Phys. France*, **47**, 693 (1986), W. Zimmermann and L. Kramer, *Phys. Rev. Lett.*, **56**, 2655 (1986), C. Oldano, *Phys. Rev. Lett.*, **56**, 1098 (1986), E. Miraldi, C. Oldano and A. Strigazzi, *Phys. Rev.*, **A34**, 4348 (1986), D. W. Allender, R. M. Hornreich and D. L. Johnson, *Phys. Rev. Lett.*, **59**, 2654 (1987), U. D. Kini, *Liquid Crystals*, **7**, 185 (1990).
[13] S. M. Arakelyan, A. S. Karayan and Y. S. Chilingaryan, *Soviet Physics Doklady*, **29**, 202 (1984).
[14] B. J. Frisken and P. Palffy-Muhoray, *Phys. Rev.*, **A 39**, 1513 (1989), *ibid*, **40**, 6099 (1989).
[15] B. J. Frisken and P. Palffy-Muhoray, *Liquid Crystals*, **5**, 623 (1989).
[16] G. Barbero, E. Miraldi, C. Oldano and P. Taverna Valabrega, *Z. Naturforsch.*, **43a**, 547 (1988).
[17] D. W. Allender, B. J. Frisken and P. Palffy-Muhoray, *Liquid Crystals*, **5**, 735 (1989).
[18] U. D. Kini, *J. Phys. France*, **51**, 529 (1990).
[19] Hp. Schad and S. M. Kelly, *Mol. Cryst. Liquid Cryst.*, **133**, 75 (1986).
[20] Hp. Schad and M. A. Osman, *J. Chem. Phys.*, **75**, 880 (1981).
[21] U. D. Kini, *J. Phys. France*, **II 5**, 1841 (1995).
[22] L. D. Landau and E. M. Lifshitz, *Electrodynamics of Continuous Media*, (Pergamon Press, 1984).
[23] As pointed out in reference 21 (see note[26] and also section 5), we do not explicitly enforce the condition of continuity of the tangential components of **E** at the boundaries $z = \pm h$. The assumption that $g \gg h$ implies that conditions at the electrodes are also being ignored. These constitute limitations of the calculations presented in this work, noting that the voltage between electrodes is assumed constant.
[24] G. Cohen and R. M. Hornreich, *Phys. Rev.*, **A 41**, 4402 (1990).
[25] P. G. Cummins, D. A. Dunmur and D. A. Laidler, *Mol. Cryst. Liquid Cryst.*, **30**, 109 (1975), J. D. Bunning, T. E. Faber and P. L. Sherrell, *J. Physique*, **42**, 1175 (1981), P. L. Sherrell and D. A. Crellin, *J. Physique Colloq. C3, suppl. no. 4*, **40**, C3-211 (1979).
[26] U. D. Kini to be published.

[27] D. Schmidt, M. Schadt and W. Helfrich, *Z. Naturforsch.*, **a27**, 277 (1975).
[28] E. Dubois-Violette, G. Durand, E. Guyon, P. Manneville and P. Pieranski, *Solid State Physics Suppl.*, **14**, 147 (1978), E. Bodenschatz, W. Zimmermann and L. Kramer, *J. Phys. France*, **49**, 1875 (1988).
[29] K. T. Schell and R. S. Porter, *Mol. Cryst. Liquid Cryst.*, **174**, 141 (1989), S. Garg, S. Saeed and U. D. Kini, *Phys. Rev.*, **E51**, 5846 (1995).
[30] S. Garg and coworkers (to be published).